Silicon–Carbide MESFET-Based 400 °C MEMS Sensing and Data Telemetry

Run Wang, Wen H. Ko, *Life Fellow, IEEE*, and Darrin J. Young

***Abstract*—A prototype high-temperature silicon–carbide (SiC) MESFET-based microelectromechanical systems (MEMS) sensing and date telemetry module is reported for harsh environment applications. The module employs a MEMS silicon capacitive pressure sensor performing pressure to frequency conversion and an on-board spiral loop serving as an inductor for the LC resonator and also as a telemetry antenna. The system demonstrates a high-temperature performance up to 400 °C, limited by the SiC MESFET characteristics, and achieves a telemetry distance of 1 m.**

***Index Terms*—High-temperature sensing, microelectromechanical systems (MEMS) sensor, silicon–carbide (SiC) MESFET, telemetry.**

I. INTRODUCTION

HIGH-TEMPERATURE wireless sensor and data telemetry systems are critical for advanced industrial, automotive, and aerospace sensing and data telemetry applications. Typical temperatures for these applications range from 200 °C to 600 °C. Higher temperatures up to and beyond 1000 °C are required for extremely harsh environments, such as turbine engines, nuclear power generators, etc. Conventional microelectronics based on bipolar junction transistors (BJT) and complimentary metal–oxide semiconductor (CMOS) technologies suffer from severe performance degradation and failure above 180 °C due to excessive leakage currents [1]. Silicon-on-insulator (SOI) technologies provide the advantage of minimized device junction areas, thus reducing the leakage current and enabling operations up to 300 °C [2]. Silicon–carbide (SiC) device technologies are promising for increased operating temperatures above 500 °C due to the wide bandgap and low intrinsic carrier concentration of the material [3], [4].

Conventional high-temperature sensing applications, such as pressure sensing, rely on using piezoresistive sensors made of silicon or SiC material [5]–[7]. These devices, however, exhibit a strong temperature dependence and suffer from contact resistance variation at elevated temperatures, substantially degrading the sensor performance because the contact resistance variation is indistinguishable from the piezoresistance change caused by the pressure information to be sensed. Capacitive sensors are attractive for high-temperature sensing due to their small temperature dependence and tolerance of contact resistance variations. However, capacitive device performance is prone to parasitic capacitances associated with the wiring and test setup. Therefore, a wireless sensing scheme is highly desirable for such applications. A high-temperature wireless capacitive sensing technique has been demonstrated by employing a resonant load-sensing method [8]. This approach eliminates any wiring parasitic capacitance, but suffers from a limited coupling distance on the order of one inch, thus undesirable for high-temperature applications. A low-power silicon-tunnel diode-based wireless transmitter achieving a telemetry distance above 1 m has been proposed for operations up to 250 °C, limited by the tunnel-diode characteristics at elevated temperatures [9]. In this paper, a high-temperature capacitive sensing and wireless data telemetry module employing an N-channel 4H-SiC MESFET from Cree Microwave, Inc., as an active device is presented. The prototype system achieves a telemetry distance of 1 m under operating temperatures up to 400 °C, limited by the MESFET characteristics. The demonstrated performance represents the highest operating temperature for semiconductor sensing and telemetry systems reported to date and is suitable for various high-temperature sensing applications. However, the high-temperature power supply problem has not yet been solved. The prototype system employs an external power supply by wire connections. Section II illustrates the high-temperature sensing and telemetry system architecture, in which design analysis with numerical examples will be given. Characteristics of passive components employed in the prototype system, including the capacitive pressure sensor, feedback capacitors, and on-board loop inductor, will be presented in Section III. Section IV shows the prototype measurement results with comparison to the expected performances.

II. HIGH-TEMPERATURE SENSING AND TELEMETRY SYSTEM

Fig. 1 presents the high-temperature prototype wireless sensing and telemetry architecture. The system consists of an N-channel 4 H-SiC MESFET LC-tuned oscillator transmitter employing a MEMS silicon capacitive pressure sensor with an on-board spiral loop inductor also functioning as a telemetry antenna. The wide bandgap and low intrinsic carrier concentration of SiC material substantially reduce the device leakage current at elevated temperatures, critical for high-temperature operations. The Colpitt's oscillator configuration is employed for the prototype design due to its simplicity. The oscillator's core electronics consist of SiC MESFET, M_1, functioning as a common-gate amplifier with a resonant circuit constituting a spiral loop inductor and a capacitive network of $\mathrm{C}_{\mathrm{sensor}}, \mathrm{C}_1$, and C_2, in which C_1 and C_2 form the feedback path. The

Manuscript received December 12, 2003; revised July 23, 2004. This work was supported in part by NASA under the Glennan Microsystems Initiative. The associate editor coordinating the review of this paper and approving it for publication was Dr. Bahram Kermani.

The authors are with the Electrical Engineering and Computer Science Department, Case Western Reserve University, Cleveland, OH 44106 USA (e-mail: rxw@po.cwru.edu; whk54@po.cwru.edu; djy@po.cwru.edu).

Digital Object Identifier 10.1109/JSEN.2005.858927

1530-437X/$20.00 © 2005 IEEE

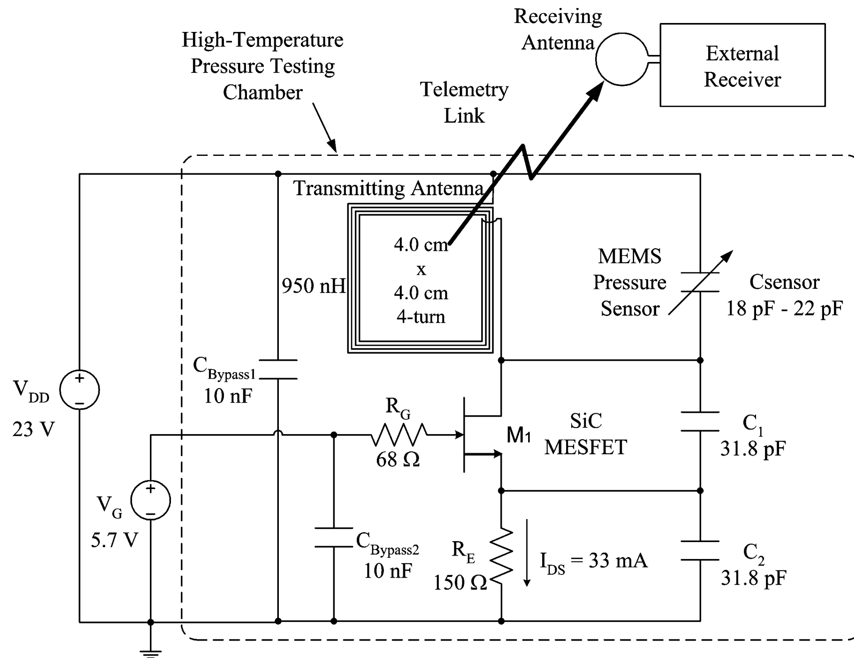

Fig. 1. High-temperature wireless-sensing architecture.

oscillator steady-state frequency is determined by the LC tank resonance, which can be expressed as

$$f_{\text{osc}} = \frac{1}{2\pi\sqrt{L\left(C_{\text{sensor}} + \frac{C_1 C_2}{C_1+C_2}\right)}}.$$

The MEMS capacitive pressure sensor converts the environment pressure information to a capacitance change, thus resulting in an oscillator output frequency variation. This frequency change can be detected by an external receiver through the telemetry link, as shown in Fig. 1. The pressure to frequency modulation scheme is attractive for achieving a reliable data transmission compared to other amplitude modulation techniques. The oscillator small-signal loop gain A_l, determined by the SiC MESFET characteristics under a proper bias condition, the values of feedback capacitors, and resonator impedance, needs to be designed large enough to ensure a reliable oscillation over a wide temperature range. The small-signal loop gain can be expressed as [10]

$$A_l = g_m \cdot [r_o \cdot (1 + g_m R_E)//R_p] \cdot \frac{1}{n}\left(1 - \frac{1}{n}\right)$$

where g_m and r_o are the small-signal transconductance and output resistance of M_1, respectively, $(1/n) = (C_1/C_1 + C_2)$, and R_p is the overall equivalent load resistance presented by the LC tank at the resonance, as will be illustrated in Section III.

Figs. 2 and 3 present the current–voltage (I–V) characteristics of the SiC MESFET measured at various temperatures. The dc bias voltages chosen are 18 V for V_{DS} and -10.2 V for V_{GS}. This bias condition results in a small transistor bias current I_{DS}, thus minimizing the oscillator power dissipation and device self-heating effect, which is critical for ensuring a reliable operation at elevated temperatures. The bias condition also corresponds to a small device output resistance. However, by a proper design, an adequate oscillator small-signal loop gain can be achieved.

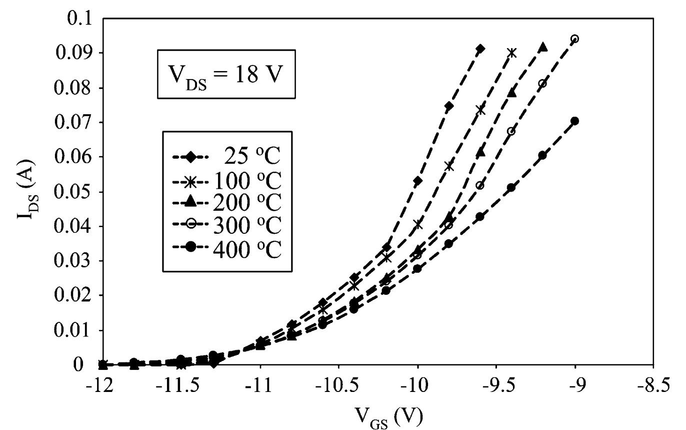

Fig. 2. SiC MESFET I_{DS} versus V_{GS} curves at various temperatures.

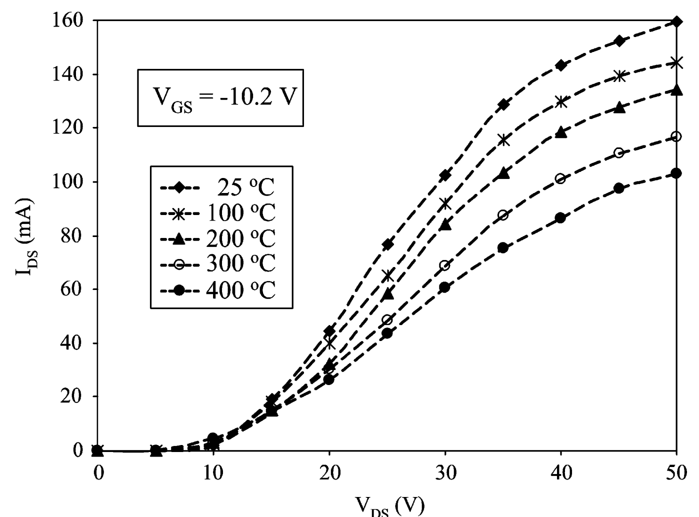

Fig. 3. SiC MESFET I_{DS} versus V_{DS} curves at various temperatures.

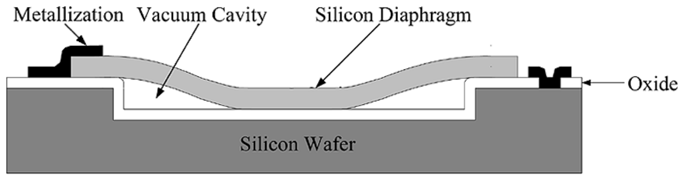

Fig. 4. Sensor cross-sectional view.

With the selected bias condition, the device dc current ranges from 33 to 21 mA at 25 °C and 400 °C, respectively. Since the threshold voltage remains nearly the same around −11.75 V, as shown in Fig. 2, the drop of current level at elevated temperatures is mainly caused by the carrier mobility degradation. As a result, the corresponding device transconductance and output resistance range from 70 mS and 200 Ω at 25 °C to 29 mS and 420 Ω at 400 °C, computed from the measured transistor I–V characteristics. Consequently, the oscillator small-signal loop gain of 5.5 at 100 °C and 4.1 at 400 °C can be achieved with a R_p value of 1 kΩ and 0.96 kΩ, respectively, as will be shown in Section III, to ensure a reliable operation over a wide temperature range. The insulation between the MESFET gate and source degrades drastically above 400 °C, thus ultimately limiting the system high-temperature performance. The bypass capacitors $\mathrm{C}_{\mathrm{bypass1}}$ and $\mathrm{C}_{\mathrm{bypass2}}$ are used to isolate any parasitic effects from the oscillator core electronics at the operating frequency and temperature. A gate resistor R_g is further employed to suppress a parasitic high-frequency oscillation mode caused by the negative resistance looking into the MESFET gate and parasitic inductance from the device package [11].

III. Passive Components

A MEMS silicon capacitive pressure sensor is employed as a demonstration vehicle for the prototype design. Fig. 4 presents a simplified cross-sectional view of the device. The sensor consists of an edge-clamped circular silicon diaphragm with a thickness of 5 μm and a radius of 400 μm over a vacuum cavity with a depth of 2.5 μm. The diaphragm deflects toward the substrate under an increasing external pressure, thus increasing the device capacitance value. Once the diaphragm touches the substrate at a designed touch point pressure, the sensor capacitance value increases near linearly with the pressure due to the linearly increasing touched area. The diaphragm thickness, radius, and cavity depth can be designed to satisfy various pressure range and sensitivity requirements [12]. The major device fabrication steps consist of: 1) a silicon substrate recess formation by reactive ion etch (RIE) followed by an oxidation process; 2) the formation of a heavily-doped boron layer (p^+ layer) at the surface of a second silicon wafer through a diffusion process; 3) wafer bonding of the silicon substrate and the second wafer in vacuum followed by a high-temperature annealing step to strengthen the bonding quality; 4) removing the backside silicon substrate material from the second wafer through a TMAH wet etch followed by patterning the p^+ diaphragm using RIE; and 5) opening contact windows and forming metal contacts. The detailed device design and fabrication process can be found in [12]. Fig. 5 shows a top view photo of a fabricated pressure sensor consisting of a circular diaphragm with an 800-μm diameter. Fig. 6 presents the measured sensor capacitance versus external pressure as a function of temperature. The device exhibits a touch point pressure of approximately 17 and 23 psi at 25 °C and 400 °C, respectively. The capacitance value changes from 18.3 pF at 5 psi to 21.8 pF at 35 psi (absolute pressure) at 25 °C, and from 18.0 pF at 5 psi to 19.9 pF at 35 psi (absolute pressure) at 400 °C. A near-linear characteristic behavior is obtained with a 1% linearity from 17 to 25 psi, and from 25 to 35 psi at 25 °C and 400 °C, respectively. The sensitivities within the linear range are 0.21 pF/psi and 0.15 pF/psi, accordingly. From the measurement, it is observed that the touch point pressure increases almost linearly with the absolute temperature. This phenomenon can be attributed to the residual air pressure trapped in the sealed cavity during the wafer bonding. An improved vacuum wafer bonding is expected to minimize the residual air trapped

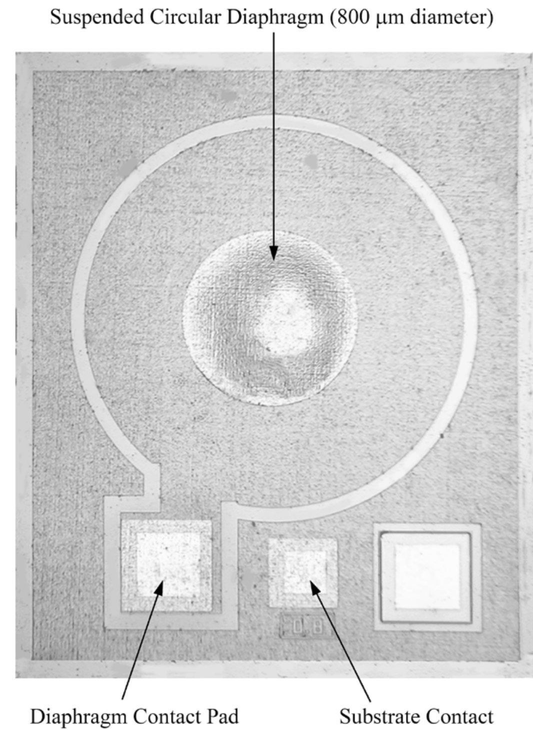

Fig. 5. MEMS pressure sensor top view.

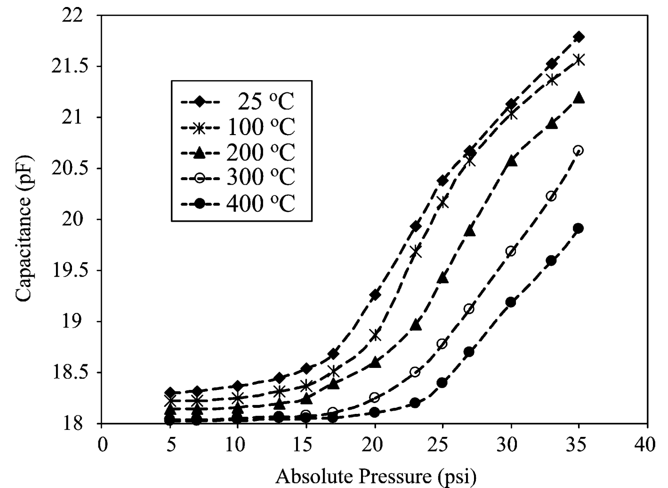

Fig. 6. MEMS pressure sensor characteristics.

in the cavity, thus minimizing this thermal effect on touch–point pressure at elevated temperatures. This processing step can be readily performed in future device fabrications.

The sensor has a measured series resistance of 27 Ω. This resistive loss of the capacitive sensor limits the oscillator operating frequency. A nominal frequency of 27 MHz in an Industrial Scientific Medical (ISM) band is, thus, chosen for the prototype design. A reduced frequency would call for an excessive spiral loop inductor dimension, limiting the system flexibility. Increased operating frequencies would demand an increased transistor bias current, hence the power dissipation and device self heating, to compensate a more pronounced sensor resistive loading effect in order to obtain an adequate oscillator loop gain.

High-temperature-grade ceramic capacitors are used for C_1 and C_2 to implement the oscillator feedback network. The capacitors have capacitance and series resistance ranging from 31.9 pF and 0.3 Ω at 25 °C to 22.4 pF and 7.6 Ω at 400 °C. Corresponding to the sensor capacitance values, a four-turn 4 × 4 cm spiral loop is designed to achieve an inductance value of 950 nH for the oscillation frequency of 27 MHz [10]. The spiral loop inductor is fabricated by a layer of 25-μm-thick gold film on a ceramic board. The inductor traces exhibit a 1 mm of width and spacing. The fabricated inductor achieves an inductance value of approximately 1.0 μH over a wide temperature range and a series resistance of 8 Ω at 25 °C and 25 Ω at 400 °C measured over a nonconducting environment. Placing the inductor over a ceramic heating substrate enclosed in a metallic testing chamber, which is a test setup for the prototype system, would result in an inductance drop from 1.0 to 0.92 μH due to the metallic environment. At the same time, the inductor series resistance changes from 8 to 10 Ω at 25 °C and 25 to 21 Ω at 400 °C. The inductance change results in an oscillation frequency increase from 27 to 28.2 MHz. The substrate and environment effects for a given setup, however, can be accurately measured and compensated in the system design. The component's temperature-dependent characteristics are also considered in the oscillator design process to ensure an adequate loop gain for a reliable oscillation startup. Based on the passive components values presented above, the overall equivalent load resistances presented by the LC tank at the resonance are 1 and 0.96 k Ω at 100 °C and 400 °C, respectively [10], which results in an adequate oscillator loop gain over the wide temperature range. The oscillator frequency can be changed from 27.4 MHz at 5 psi to 28.8 MHz at 35 psi (absolute pressure) at 25 °C and from 30.3 to 31.3 MHz over the same pressure range at 400 °C, which closely matches the measurement results as will be presented in Section IV. An increased operating frequency can be obtained with redesigned low-loss capacitive sensors, thus reducing the spiral inductor dimension which is attractive for further system miniaturization. Low-loss capacitive sensors and spiral inductors are also important for minimizing the required dc bias current of the MESFET, thus reducing the system power dissipation.

IV. Experiment Results

Fig. 7 shows a photo of the prototype wireless MEMS sensing and data telemetry system. The SiC MESFET, MEMS capacitive pressure sensor, resistors, and capacitors are attached to a through-hole ceramic substrate and gold-wire bonded to form the prototype system. High-temperature-grade bias resistors and bypass capacitors are used to ensure a reliable high-temperature operation. The SiC MESFET is housed in a flange-mount package designed for high-power and high-frequency operations. All components are located at the center of the spiral loop for a compact design. Such a layout configuration causes a negligible effect on the inductance value and quality factor of the spiral loop with in the operating frequency range, thus maintaining the designed oscillator frequency. Fig. 8 shows the experiment setup for the prototype module. The sensor telemetry system is positioned inside a pressure-testing chamber with temperatures elevated and controlled through a ceramic heating substrate. A spectrum analyzer is used as an external receiver with a tuned spiral loop connected to the input port as a receiving antenna. In the future, a custom designed receiver consisting of a phase-locked loop will be employed for retrieving the incoming sensor information. The oscillator operates around 28.6 MHz under 1 atm at 25 °C and can be varied over 1.3 MHz through a pressure increase from 5 to 35 psi (absolute pressure), as shown in Fig. 9. The measurement shows a near linear characteristic

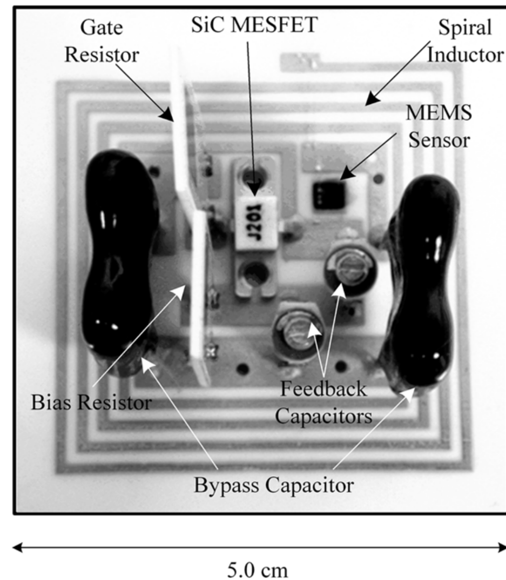

Fig. 7. Prototype board photo.

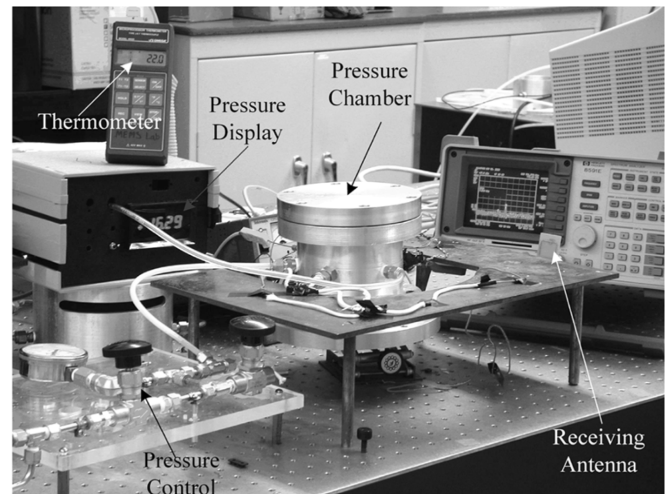

Fig. 8. Experiment setup.

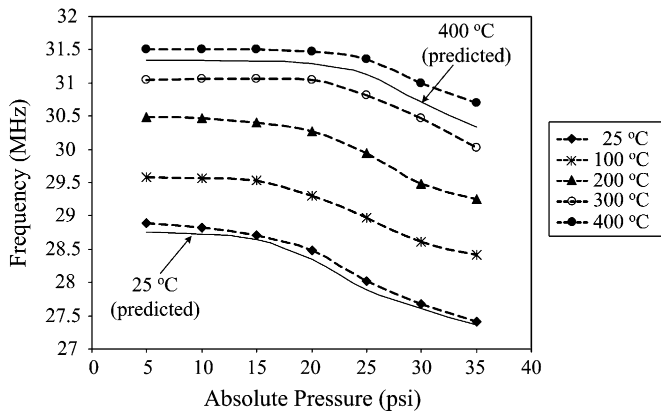

Fig. 9. Pressure versus frequency.

behavior between 17 and 27 psi with a linearity of 1% and a sensitivity of 65 kHz per psi at 25 °C. For a relaxed linearity of 3%, an extended linear region from 15 to 35 psi can be obtained. At 400 °C, the oscillator operates around 31.5 MHz under 1 atm and varies over 800 KHz through a pressure increase from 5 to 35 psi (absolute pressure). A 1% linearity range is achieved between 27 to 35 psi with a sensitivity of 66 kHz per psi. Fig. 9 also presents the predicted system responses at 25 °C and 400 °C, respectively, shown by the solid-line curves, indicating a close match to the experimental data. The demonstrated performance represents the highest operating temperature for semiconductor sensing and telemetry systems reported to date and is suitable for various high-temperature sensing applications.

At a constant pressure, the oscillator exhibits a frequency shift of approximately 2.6 MHz over the temperature range from 25 °C to 400 °C due to the components temperature dependence. An added temperature sensor, thus, will be required in a practical application to calibrate the system with a lookup table or a functional curve fit to minimize the thermal effect. A high-temperature silicon-based spreading-resistance temperature sensor can be incorporated with the proposed system for the calibration [13]. Fig. 10 presents the received power versus telemetry distance under 1 atm measured at 25 °C, 100 °C, 200 °C, 300 °C, and 400 °C, respectively, indicating that the spectrum analyzer can receive an incoming signal with a power of at least −105 dBm over a telemetry distance of 1 m. Fig. 11 shows the corresponding received power spectrum at 1-m telemetry distance with an SNR of 10 dB from the prototype oscillator operating at 400 °C. The receiver noise floor limits the achievable telemetry distance. An extended communication range is expected with a more sensitive receiver. It is found that positioning the transmitting and receiving coil loops in a coplanar manner can result in a stronger incoming signal than axially-aligned loops with an approximately 10-dB improvement beyond a telemetry distance of 30 cm. It is also observed that placing the sensor and data telemetry module inside the metal testing chamber would enhance the incoming signal strength by approximately 2 dB compared to positioning over a wood bench. This enhancement is likely due to the metallic chamber acting as a large radiating antenna. Movement of any nearby metallic objects has a negligible effect on the telemetry performance.

The prototype system exhibits an initial oscillation frequency drift of approximately 21 and 85 kHz under 1 atm measured continuously over 30 min after being activated at 25 °C and 350 °C,

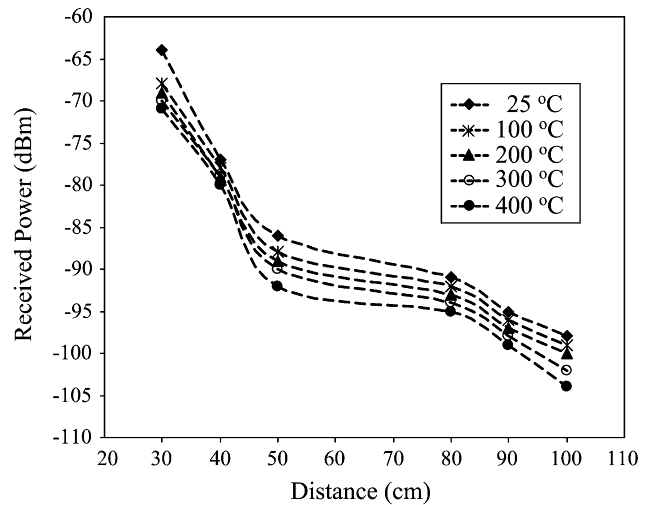

Fig. 10. Received power versus distance.

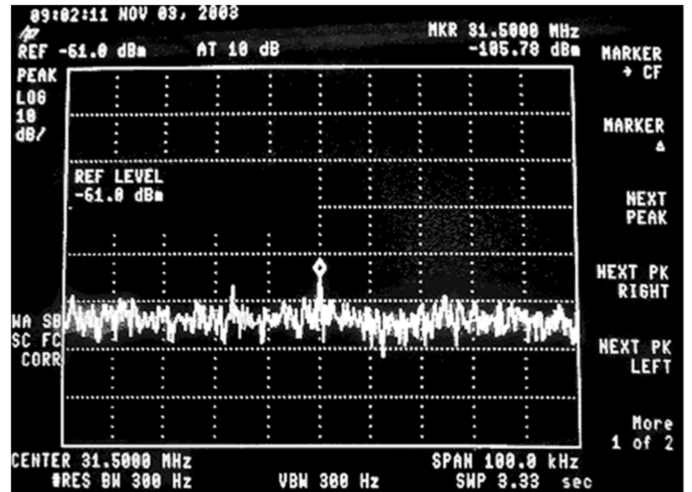

Fig. 11. Received power spectrum.

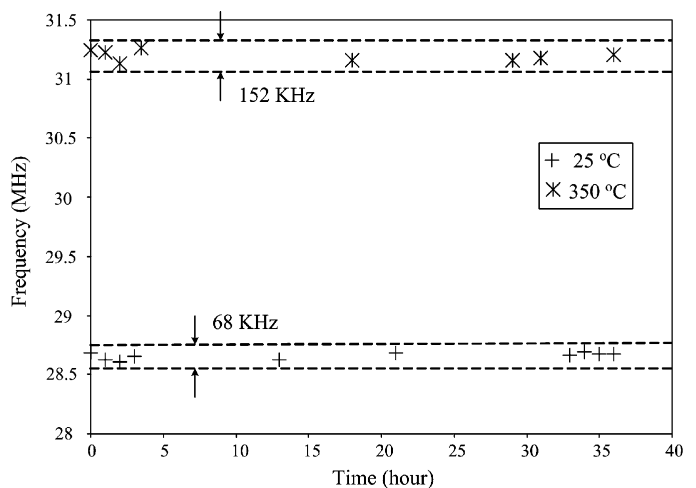

Fig. 12. Oscillator frequencies at fixed temperatures over time.

respectively. This results in a sensing resolution of 0.16 psi (11 mbar) at 25 °C and 0.63 psi (43 mbar) at 400 °C within the linear range. The oscillator frequency measured at different times within a 36-h period shows a peak to peak frequency variation of 68 and 152 KHz at 25 °C and 350 °C, respectively, as shown in Fig. 12, which indicates that the system can achieve

a sensing repeatability of 0.52 (36 mbar) and 1.1 psi (76 mbar) at the corresponding temperatures. This frequency variation can be possibly caused by the components characteristics variation due to the temperature cycling over time.

V. Conclusion

SiC MESFET-based oscillator transmitter is attractive for high-temperature MEMS sensing and data telemetry applications. The prototype wireless sensing and communication module achieves high-temperature operations up to 400 °C over a telemetry distance of 1 m, which is suitable for various harsh environment-sensing applications. Although an external power supply is required for the prototype system, the propose architecture can substantially reduce the system output wiring complexity for potential sensing array and network applications. The silicon-based capacitive pressure sensor employed in the prototype design is functional at 400 °C. The system high-temperature performance is limited by the SiC MESFET characteristics.

References

[1] J. Goetz, "Sensors that can take the heat," *Sensors*, pp. 20–38, Jun. 2000.

[2] A. J. Auberton-Herve, "SOI: Materials to systems," in *Proc. Int. Electron Devices Meeting*, 1996, pp. 3–10.

[3] D. M. Brown, M. Ghezzo, J. Kretchmer, V. Krishnamurthy, G. Michon, and G. Gati, "High temperature silicon carbide planar IC technology and first monolithic SiC operation amplifier IC," in *Proc. 2nd Int. High Temperature Electronics Conf.*, 1994, pp. XI–17–XI–17.

[4] P. G. Neudeck, R. S. Okojie, and L.-Y. Chen, "High temperature electronics—A role for wide bandgap semiconductors?," *Proc. IEEE*, vol. 90, pp. 1065–1076, Jun. 2002.

[5] C.-H. Wu, S. Stefanescu, H.-I. Kuo, C. A. Zorman, and M. Mehregany, "Fabrication and testing of single crystalline 3C-SiC piezoresistive pressure sensors," in *Proc. 11th Int. Conf. Solid State Sensors and Actuators*, 2001, pp. 514–517.

[6] A. A. Ned, R. S. Okojie, and A. D. Kurtz, "6H-sic pressure sensor operation at 600°C," in *Proc. 4th Int. High Temperature Electronics Conf.*, vol. 14, 1998, pp. 257–260.

[7] R. S. Okojie, A. A. Ned, and A. D. Kurtz, "Operation of a (6 H)-SiC pressure sensor at 500°C," in *Proc. Inf. Conf. Solid-State Sensors and Actuators Tech. Dig.*, 1997, pp. 1407–1409.

[8] M. A. Fonseca, J. M. English, M. V. Arx, and M. G. Allen, "Wireless micromachined ceramic pressure sensor for high-temperature applications," *J. Microelectromech. Syst.*, vol. 11, no. 3, pp. 337–343, Sep. 2002.

[9] M. Suster, W. H. Ko, and D. J. Young, "Optically-powered wireless transmitter for high-temperature MEMS sensing and communication," in *Proc. 12th Int. Conf. Solid-State Sensors and Actuators Tech. Dig.*, Jun. 2003, pp. 1703–1706.

[10] T. H. Lee, *The Design of CMOS Radio-Frequency Integrated Circuits*. Cambridge, U.K.: Cambridge Univ. Press, 1998.

[11] U. Karacaoglu and I. D. Robertson, "MMIC active bandpass filters using varactor-tuned negative resistance elements," *IEEE Trans. Microwave Theory Tech.*, vol. 43, no. 12, pp. 2926–2932, Dec. 1995.

[12] W. H. Ko and Q. Wang, "Touch mode capacitive pressure sensors," *Sens. Actuators*, vol. 75, pp. 242–251, 1999.

[13] B. Li, P. T. Lai, C. L. Chan, and J. K. O. Sin, "Optimization of silicon spreading-resistance temperature sensor," in *Proc. Electron Devices Meeting*, Hong Kong, 2000, pp. 20–23.

Run Wang was born in China in 1980. She received the B.S. degree from the Department of Electronic Engineering, Tsinghua University, Beijing, China, in 2001, and the M.S. degree from the Department of Electrical Engineering, Case Western Reserve University (CWRU), Cleveland, OH, in 2004. She is currently pursuing the Ph.D. degree at the Department of Electrical Engineering, CWRU.

Her primary research interests is semiconductor material and device characterizations.

Wen H. Ko (LF'90) received the B.S.E.E. degree from Xiamen University, China, in 1946, and the M.S. and Ph.D. degrees in electrical engineering from the Case Institute of Technology, Cleveland, OH, in 1956 and 1959, respectively.

He was a faculty member of the Electrical Engineering and Biomedical Engineering Departments, Case Western Reserve University (CWRU), Cleveland, 1959 to 1993. He became a Professor Emeritus in electrical engineering at CWRU in July 1993. He holds 21 patents and has authored 317 publications, 131 of which are in referenced journals, in the areas of solid state electronics, microsensors and actuators, biomedical instrumentation, implant electronics, and control system design.

Dr. Ko is a Fellow of the American Institute of Medical and Biological Engineering. He received the Career Achievement Award at the Transducer 1997 Conference, Chicago, IL. He is on the editorial boards of *Sensors and Actuators* and *Micro-system Technologies* and was on the editorial boards of *Telemetry and Patient Monitoring* (1974–1984) and *Medical Progress Through Technology* (1983–1988). He was the Chairman of the International Steering Committee on Solid-State Sensors and Actuators Conferences from 1983 to 1987 and the Chairman of the International Steering Committee on Chemical Sensor Meetings from 1991 to 1993. He is the President of the Transducer Research Foundation that has sponsored the Hilton Head Workshops on Sensors and Actuators in America since 1992.

Darrin J. Young received the B.S., M.S., and Ph.D. degrees from the Department of Electrical Engineering and Computer Sciences, University of California, Berkeley, in 1991, 1993, and 1999, respectively.

He joined the Department of Electrical Engineering and Computer Science, Case Western Reserve University, Cleveland, OH, as an Assistant Professor in 1999. His research interests include MEMS and nanoelectromechanical devices design, fabrication, and integrated analog circuit design for communications, inertial sensing, biomedical implants, and general industrial applications.